



Shear Strength of Rock Fractures Under Dry, Surface Wet and Saturated Conditions

Bo Li¹ · Xinna Ye¹ · Zihao Dou² · Zhihong Zhao² · Yingchun Li³ · Qiang Yang⁴

Received: 11 August 2019 / Accepted: 30 January 2020 / Published online: 11 February 2020
© Springer-Verlag GmbH Austria, part of Springer Nature 2020

Abstract

For rock fractures, the degradations in the strength of contacting asperities and the surface frictional resistance are responsible for the water-induced weakening in the shear strength. To quantitatively examine their independent roles, direct shear tests on sawtooth fracture samples of granite and sandstone under three moisture conditions: dry, surface wet and saturated, were conducted subject to three levels of normal stresses. The surface wet condition only resulted in the variation in the basic friction angle and the saturated samples underwent the degradation in both unconfined compressive strength (UCS) and basic friction angle, which were obtained via unconfined compression test and direct shear test, respectively. Two weakening coefficients that represent the reductions in UCS and basic friction angle, respectively, were proposed and incorporated into an analytical model, which quantifies the entire shear stress evolutions during shear based on a continuous yielding mechanism. The difference in the shear strength between dry and surface wet conditions originates from the lubricant effect of water represented by the change in basic friction angle with a weakening coefficient less than 10% for both rocks. Under the saturated condition, the weakening coefficient of the UCS varies significantly from 15.17% for granite to 50.39% for sandstone. A series of datasets that characterize the reductions in UCS and basic friction angle induced by water were collected from the literature, which were then incorporated into the analytical model to estimate the general weakening trend in the shear strength of the common rocks in practices. For crystalline rocks, the water-mediated lubrication seems to be the primary mechanism reducing the shear strength, while for sedimentary rocks, the remarkable degradation in UCS may dominate the weakening mechanism. The quantified weakening coefficients and the revealed weakening behavior of various rocks can be directly linked to the fracture shear strength estimation in engineering design.

Keywords Rock fracture · Water · Shear strength · Weakening · Direct shear test · Analytical model

1 Introduction

Water is one of the most important environmental factors affecting the deformation and failure behaviors of fractured rocks in engineering practices such as slopes, tunnels and mining (Jaeger et al. 2007). Numerous experimental studies

have been carried out to quantitatively characterize the effect of water on the mechanical properties of various rocks (Lajtai et al. 1987; Feucht and Logan 1990; Karfakis and Askram Karfakis and Akram 1993; Dove 1995; Feng et al. 2001; Li et al. 2003; Nara et al. 2010; Wasantha and Ranjith 2014; Cherblanc et al. 2016; Hua et al. 2016; Wong et al. 2016; Zhao et al. 2017a, 2019a; Qiao et al. 2017). The reductions in the unconfined compressive strength (UCS), elastic modulus and tensile strength of the clay-bearing rocks can be up to 90%, 93% and 90%, respectively, with water content from oven-dried to saturated conditions (Erguler and Ulusay 2009). Similar level of reduction (around 70%) has also been reported for Carbonate rocks (Rajabzadeh et al. 2012). Comparatively, crystalline rocks demonstrate good quality in resisting the water-induced degradation which typically exhibits a reduction ratio less than 10% (Wong et al. 2016). The presence of water also leads to a greater

✉ Zhihong Zhao
zhzhao@tsinghua.edu.cn

¹ Key Laboratory of Rock Mechanics and Geohazards of Zhejiang Province, Shaoxing 312000, China

² Department of Civil Engineering, Tsinghua University, Beijing 100084, China

³ State Key Laboratory of Coastal and Offshore Engineering, Dalian University of Technology, Dalian 116024, China

⁴ Department of Hydraulic Engineering, Tsinghua University, Beijing 100084, China

strain at failure, which becomes more obvious under greater confining pressures (Lockner 1995). These examples suggest a strong need in comprehensively understanding the weakening effects of water on different rocks to efficiently assist engineering design.

The magnitudes of the water-induced degradation of rocks are dependent on the properties of both fluids and rocks, as well as time. The chemical reactions can happen more efficiently when immersed for a longer time in a solution with higher concentration of H^+ , thereby making the rock samples softer and more ductile (Li et al. 2003). The more water sensitive constituents such as clay and silt a rock contains, the greater level the degradation may happen. The extent of activated cracking of rocks in aqueous solution is dependent on the micro-structure and mineralogical make-up of the rock as well as the chemistry of the solution (Karfakis and Akram 1993). For the rocks mainly consisting of quartz and feldspar, the water–rock reactions result in the reduction of cohesive strength only, while the friction angle is almost unaffected. If rocks contain certain amounts of clay or silt, both of the cohesive strength and the friction angle will be reduced by the saturation (Li et al. 2005). Two distinct types of bonding within calcarenites are identified: temporary bonding and persistent bonding, which are responsible for the observed rapid decrease in rock strength when water fills the pores (a short-term effect), and a long-term weakening of saturated rocks (a long-term effect) (Ciantia et al. 2015a, b). Previous studies suggested four possible mechanisms responsible for the water-induced degradation of intact rocks (Van Eeckhout 1976; Baud et al. 2000; Zhao et al. 2017a): (1) fracture energy reduction (Lajtai et al. 1987; Dove 1995; Nara et al. 2010), (2) capillary tension decrease, (3) frictional reduction (Feucht and Logan 1990) and (4) chemical and corrosive deterioration (Feucht and Logan 1990; Feng et al. 2001; Li et al. 2003).

Compared with the extensive studies on the water-induced degradation of intact rocks, the number of studies on the influence of water on the mechanical properties of rock fractures, particularly the fracture shear strength, is limited. Previous studies revealed a reduction trend in the fracture friction angle of various rock types under wet conditions (Li et al. 2005; Gutierrez et al. 2000; Ulusay and Karakul 2016; Kim and Jeon 2019). For example, experiments on the marl fractures demonstrated a strong dependency of shear strength on the water content, i.e., the friction angle drops from 22° for a dry fracture to 12° for a saturated fracture, and the fracture cohesion decreases from 0.41 MPa under dry conditions to 0.32 MPa under wet conditions (Pellet et al. 2013). Another test on sawtooth sandstone fractures revealed a reduction ratio of 20–24% of the peak shear strength due to wetting (Zhao et al. 2017b). The moisture condition also alters the surface morphology of various fracture types after being immersed in in situ solutions (Chen et al. 2014). The

introduction of water into rock fractures may modify the mechanical properties in two ways: (1) a purely mechanical effect of pore pressure, i.e., the classical effective stress principle, and (2) physicochemical interactions between water and fracture walls, including lubrication, softening, argillation, scouring and pressure solution (Zhao et al. 2018a). Even though a few theoretical models have been developed to describe the physico-chemically mediated changes in fracture aperture (Yasuhara et al. 2004; Liu et al. 2006; Min et al. 2009), the criteria for fracture shear strength under different wetting conditions have not been reported to the authors' knowledge.

It has been well understood that the shearing resistance along rock surfaces arises from two components: the basic frictional resistance of the two flat surfaces determined by the rock material, and the resistance offered by the roughness on the fracture surface (Barton 1971). The basic frictional resistance can be represented by a basic friction angle (ϕ_b) that is commonly estimated by tilt test or shear test on flat rock surfaces. This angle typically ranges from 20° to 40° for different types of rocks and the wet samples exhibit a reduction of 0 – 10° comparing to the dry samples (Alejano et al. 2012). The degradation of intact rock when wetted decreases the strength of asperities, which together with the reduction in ϕ_b leads to the decreasing shear strength. On the other hand, a great number of methods and parameters have been developed for characterizing the surface roughness such as the joint roughness coefficient (JRC), statistical parameters, fractal dimensions, and wavelet analysis (e.g., Barton and Choubey 1977; Grasselli et al. 2002; Jiang et al. 2014; Li et al. 2008; Zou et al. 2015). These parameters have been successfully incorporated into different criteria for estimating the shear strength of rock fractures (e.g., Barton 1982; Saeb and Amadei 1992; Indraratna et al. 2015; Li et al. 2018). The effect of water on the variation in surface morphology happens very slowly especially for crystalline rocks that may be negligible when fresh rocks are mainly concerned. Therefore, the changes in the strength of asperities and the basic friction angle induced by water are considered as the two primary factors that influence the shear behavior of wetted rock fractures.

To date, however, the existing studies mainly focused on the effects of water on the intact rock strength and the basic friction angle of fractures separately. None of them, if any, have developed mechanical models that link these two factors together and taken into account the entire wear process on asperities during shear to systematically estimate the change of peak and residual shear strengths induced by water. Except the dry and saturated conditions, water flowing into dry fractures that only wets the surface has been frequently encountered in rock engineering, the effect of which on the shear behavior has not received sufficient investigation in the past. In light of these, this study conducted

direct shear tests on granite and sandstone fracture samples under three distinct moisture conditions: dry, surface wet, and saturated, subject to three levels of normal stresses. A mechanical model that formulates the continuous yielding of contacting asperities in terms of shear-off was introduced to calculate the entire shear stress evolution of the tested fractures. The reductions in the UCS and ϕ_b required in the calculation were obtained through unconfined compression test on cylindrical samples and direct shear test on flat fracture surfaces, respectively. After verification, this model was applied to the collected datasets of seven types of rocks reported in literature to estimate their fracture shear strength under different moisture conditions. This study provides a general understanding of the weakening shear strength of rock fractures when wetted from the engineering viewpoint by introducing two weakening coefficients to represent the reduction in the fundamental shear resistance components, which may benefit the engineering design when wetting conditions are encountered.

2 Experimental Methods

2.1 Sample Preparation

It is well understood that rocks with different mineral compositions can have significantly different responses to water. We selected granite and sandstone that are extensively encountered in engineering practices in this generic study. The granite was collected from Beishan, China, a potential

site for high-level radioactive waste repository. A random 300-point modal analysis of three thin-sections showed that the Beishan granite is composed of 30% quartz, 35% plagioclase, 25% alkali feldspar, 6% biotite and 4% muscovite in volumetric fraction. Most grains range between 0.1 and 0.2 mm in size. The sandstone is composed of 40% quartz, 36% feldspar, 21% debris (e.g., tuff and andesite) and 3% clay in volumetric fraction. It is fine-grained with most grain sizes smaller than 0.06 mm. Since this study primarily focuses on the effect of wetting on the shear strength of fractures, the underlying weakening mechanisms such as bonding decay among minerals are referred to related literature (Nara et al. 2010; Ciantia et al. 2015a, b; Zhao et al. 2017b).

To assess the influence of water on the shear behavior of rock fractures, it is essential to understand the change of fundamental mechanical properties of rocks before and after wetting. In the experiment, we prepared four types of samples: (1) cylindrical intact samples, (2) cubic fracture samples with flat surfaces, (3) cubic fracture samples with triangularly shaped sawtooth asperities, and (4) cubic fracture samples with rough-walled surfaces (Fig. 1). The cylindrical intact samples have a diameter of 5 cm and a height of 10 cm and the cubic fracture samples have a side length of 5 cm. The cubic fracture samples of type (2) were axially cut and polished to create flat surfaces for determining the basic friction angle. The samples of type (3) were saw-cut to form regular triangularly shaped asperities. The height for each triangular asperity is 2 mm and the inclination angle is 45°. The rough-walled fracture samples [type (4)] were generated

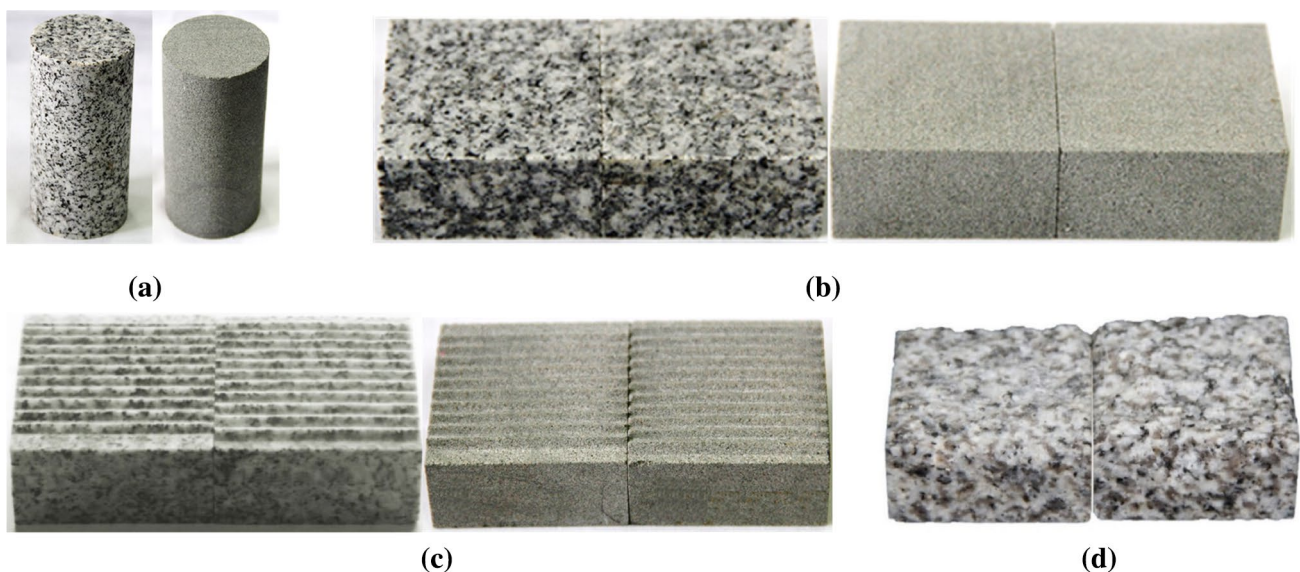


Fig. 1 Photographs of examples of the tested granite and sandstone samples. **a** Cylindrical intact rock samples; **b** fracture sample with flat surfaces; **c** sawtooth fracture samples; **d** tensile granite frac-

ture samples. In (a–c), the left and right samples are granite and sandstone, respectively

by axially splitting intact rock blocks, analogous to Brazilian test, which represent fresh tensile fractures existing in nature.

It is notable that even for split fractures in laboratory under well-controlled stress environment, the created fractures still exhibit different degrees of roughness, which may yield a wide range of shear strengths under the same moisture condition due to the randomness and non-stationarity of surface characteristics. The fractures with regular asperities were preferentially selected over rough-walled fractures because the uncertainties introduced by the roughness may mask the actual effect of wetting especially for crystalline rocks that suffer from a limited strength degradation when saturated.

The cylindrical samples were divided into two groups that were oven-dried and fully saturated, respectively. The dry samples were heated by placing the samples in oven for 24 h under a constant temperature of 60 °C. The other group was immersed in distilled water and was placed in a sealed canister subject to a vacuum pressure of 10 Pa for 3 days to achieve a complete saturation. The water–rock reaction is sensitive to the temperature and its magnitude depends on the reacting time (Yasuhara et al. 2004). Here, we kept all samples at room temperature that is commonly encountered in the field. The saturation time of 3 days indicates that the samples have undergone the initial stage of reaction, resulting in the weakening of rocks that is typically fiercer than the following (Zhao et al. 2017a). The test results shown below revealed that a short period of 3 days still caused remarkable degradation of the rock strength. We leave the influences of temperature and immersed time to the next stage of research.

For the fracture samples, except the completely dry and saturated conditions, we considered another moisture condition where only the fracture surfaces are wet while the matrix is dry, referred to as surface wet condition (Fig. 2b). This condition represents some water-injection or seepage related practices such as hydraulic fracturing in dry rocks and rock slopes subject to occasional rainfall. The shear test was conducted immediately after the surfaces were wetted to ensure that chemical reaction mediated degradation is negligibly small. Therefore, the physical lubrication effect of water on the sliding that may change the basic friction angle can be effectively estimated under this condition.

Three samples were prepared for each moisture and mechanical boundary condition to eliminate the testing errors and ensure the repeatability of test, leading to 12 cylindrical samples and 108 cubic samples in total.

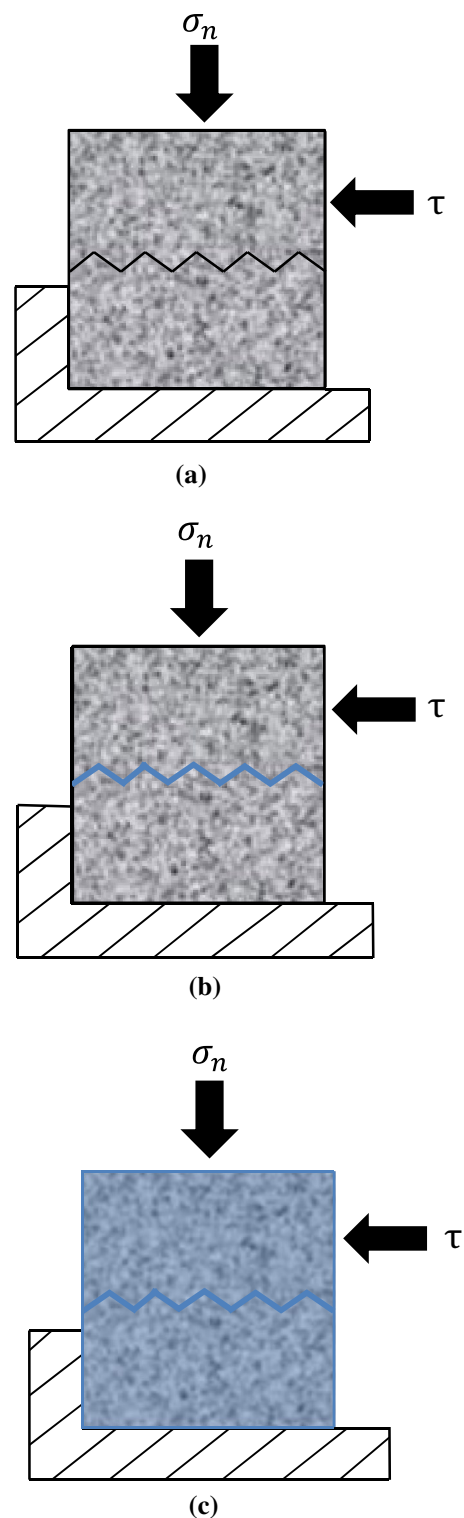


Fig. 2 Schematic view of shear tests under (a) dry, (b) surface wet, and (c) saturated conditions. Water is indicated by the blue color

2.2 Experimental Procedure

The mechanical properties of granite and sandstone were determined through unconfined compression tests on dry and saturated cylindrical samples, following the ISRM suggested method for determining the UCS and deformability of rock materials (Ulusay and Hudson 2007).

The direct shear test was performed on dry, surface wet, and saturated samples with a servo-controlled shear apparatus (YZW-50, Zhao et al. 2019b). Shear and normal loads are applied by servo-controlled hydraulic jacks. The normal load is perpendicular to the fracture plane and transferred to the sample via a spherical junction and the horizontal motion is guided by a precision linear bearing, which is designed for low friction and a single degree of freedom. This ensures that during shearing, the upper sample holder can move with a minimum friction and bending moment. High precision vertical and horizontal measurements of the sample displacements are provided by two vertical LDVTs and two horizontal LDVTs, respectively, directly attached to the sample. Fracture samples were fixed into the upper and lower shear boxes and normal stresses of 2 MPa, 5 MPa and 10 MPa, respectively, were applied to the samples. For samples under surface wet and saturated conditions, the samples were placed in a water tank during test that ensured the fracture void spaces were filled with water (Fig. 2). The samples were then sheared at a displacement rate of 0.5 mm/min, and the shear displacement and shear stress were accurately measured and recorded via a PC equipped with a data-acquisition system. Before and after each shear test, the morphology of the fracture surface was measured using a laser scanner (OKIO-5M, TENYOUN). To examine the shear-induced damage on fracture surfaces, we transformed the digitized surfaces before and after shear to the same coordinate system and calculated the changes in asperity heights (Zhao et al. 2018b). To obtain the basic friction angle of granite and sandstone fractures under different moisture conditions, direct shear tests were conducted on fracture samples with flat surfaces following the same procedure described above.

3 Analytical Method

Li et al. (2018) developed an analytical model to predict the shear behavior of rough-walled rock fractures and quantify the deterioration of two-order asperities. The surface roughness was quantitatively decomposed into waviness and unevenness as recommended by ISRM (2007), and the measurable geometric properties such as asperity wavelength and angle were used for shear behavior estimation. This model, comparing to previous models that are merely applicable to regular-shaped asperities (Saeb and Amadei 1992; Indraratna et al. 2005) and those based on statistical parameters

(e.g., JRC) (Indraratna et al. 2015), can better represent the role played by the asperities of different sizes and the entire evolution of shear stress in a shear process. Here, we introduced two weakening coefficients β_s and β_f that represent the reduction ratio in UCS and ϕ_b , respectively, to this analytical model to estimate the effect of moisture condition on the fracture shear strength. Only key aspects of this method are presented below, and details are available in Li et al. (2017, 2018).

A surface profile with roughness is characterized by the waviness and the unevenness, which are quantified by the inclination angle (i_w), wavelength (λ_w) and amplitude (A_w) of the waviness, and the inclination angle (α_u), wavelength (λ_u) and amplitude (A_u) of the unevenness (Li et al. 2017, 2018).

The total shear resistance is composed of the waviness and unevenness that represent the effect of roughness, and the basic friction of a fracture surface. Therefore, the mobilisable shear stress, τ^m , can be written as:

$$\tau^m = \sigma_n \tan [(1 - \beta_f)\phi_b + i_d^m + \alpha_d^m](1 - a_s) + a_s\sigma_s \tag{1}$$

where, β_f is the weakening coefficient for the basic friction angle ϕ_b , i_d^m is the mobilisable asperity angle for the waviness, α_d^m is the mobilisable asperity angle for the unevenness, and σ_s is the shear stress required to shear-off an asperity. The sheared-off area ratio, a_s , of waviness and unevenness is:

$$a_s = \frac{a_s^w + a_s^u}{S_0^w + S_0^u} \tag{2}$$

where a_s^w and a_s^u denote the sheared area of waviness and unevenness, respectively, and S_0^w and S_0^u represent the initial area of waviness and unevenness, respectively.

The dilation angles of waviness and unevenness at step i , $i_d(i)$ and $\alpha_d(i)$ are written as:

$$\tan i_d(i) = \frac{e^{-c_w(i)W_s^p(i)}}{2 - e^{-c_w(i)W_s^p(i)}} \tan i_d(i - 1) \tag{3}$$

$$\tan \alpha_d(i) = \frac{e^{-c_u(i)W_s^p(i)}}{2 - e^{-c_u(i)W_s^p(i)}} \tan \alpha_d(i - 1) \tag{4}$$

where c_w and c_u are the degradation coefficients for the critical waviness and unevenness, respectively.

The classic wear theory suggests that the volume of sheared-off asperities is a function of the normal stress, shear displacement and surface roughness degree (Barwell 1958; Queener et al. 1965). Here, we improve the original model developed by Li et al. (2018) by linking the evolution of asperity area to a function of the plastic work and the remaining asperity area. The increment of the sheared asperity area at step i , $\Delta S_s(i)$, over an increment of plastic work, $\Delta W_s^p(i) = \tau \Delta \delta_s^p(i)$, is presumed to be linearly proportional to

the asperity area available for shear at step i , equal to the un-sheared asperity area at the last step $S(i-1)$:

$$\frac{\Delta S_s(i)}{\Delta W_s^p(i)} = c(i)S(i-1) \tag{5}$$

where $c(i)$ is the degradation coefficient of the asperity at step i , and $S(i-1) = \lambda(i-1)A(i-1)/2$. λ is the wavelength and A is the amplitude for waviness or unevenness.

The sheared asperity area at step i is:

$$S_s(i) = S(i-1) - S_b(i) \tag{6}$$

where $S_b(i)$ is the un-sheared asperity area before experiencing the increment in dilation $\Delta\delta_n(i)$ over step i . The sheared areas of waviness and unevenness at step i , $S_s^w(i)$ and $S_s^u(i)$ can be written as:

$$S_s^w(i) = \frac{\lambda_w(i-1)}{2} \left[A_w(i-1) - \frac{\lambda_w(i-1)}{\cot i_d(i) + \cot i_0} \right] \tag{7}$$

$$S_s^u(i) = \frac{\lambda_u(i-1)}{2} \left[A_u(i-1) - \frac{\lambda_u(i-1)}{\cot \alpha_d(i) + \cot \alpha_0} \right] \tag{8}$$

respectively, where i_0 is the initial inclination angle of the waviness and α_0 is the initial inclination angle of the unevenness.

The degradation coefficients of waviness and unevenness at step i , $c_w(i)$ and $c_u(i)$ are:

$$c_w(i) = k \frac{i_d(i)}{(1 - \beta_s)\sigma_c \sqrt{S_w(i-1)}} \tag{9}$$

$$c_u(i) = k \frac{\alpha_d(i)}{(1 - \beta_s)\sigma_c \sqrt{S_u(i-1)}} \tag{10}$$

where k is a dimensionless coefficient that represents the effect of experimental environments such as temperature on the asperity degradation that is constant here. β_s is the weakening coefficient for the UCS, i.e., σ_c . Rocks with a smaller strength can be more fiercely damaged due to wear.

To present the decay of shear stiffness after the failure of contacting asperities, a stiffness reduction factor, F , is introduced as (Itasca Consulting Group Inc. 2011):

$$F = 1 - \frac{\tau}{\tau^m} \tag{11}$$

Fk_s represents the present shear stiffness at given mobilisable shear stress, and τ is the actual stress. The shear stress can then be updated by:

$$\tau(i) = \tau(i-1) + Fk_s \Delta\delta_s \tag{12}$$

where $\Delta\delta_s$ is the increment of shear displacement. In the elastic stage where the failure of contacting asperities has not happened, the value of F is taken as 1.

The original model has been validated against the experimental data on both artificial and natural fractures of different rocks under varying initial normal stresses and normal stiffness (Li et al. 2017, 2018). For the fractures with saw-tooth asperities, the unevenness that represents small or secondary scale roughness vanishes and all the terms associated with the unevenness can be simply removed from the calculation. The geometric measurement for the critical waviness and critical unevenness of rough-walled fractures follows the approach of Li et al. (2017). The values of σ_c and ϕ_b under the dry condition and their corresponding weakening coefficients β_s and β_f under wetting conditions are determined by the experiments mentioned above.

4 Results

4.1 Unconfined Compressive Strength and Basic Friction Angle

Through the unconfined compression test, the mean value and the standard deviation (SD) of UCS for granite and sandstone were obtained as tabulated in Table 1. The specific values for granite are 157.93 MPa with a SD of 2.83 MPa under dry conditions and 133.97 MPa with a SD of 12 MPa under saturated conditions. The values for sandstone are 76.60 MPa with a SD of 8.16 MPa under dry conditions and 38 MPa with a SD of 1.15 MPa under saturated conditions. The weakening coefficients β_s are 15.17% and 50.39% for granite and sandstone, respectively. These results conform to the general behavior of granite and sandstone in dry and saturated conditions, which are in concert with the fact that the crystalline rocks have better resistance to the water-induced degradation (Wong et al. 2016).

The evolutions of shear stress during shear tests on the flat fracture samples under dry, surface wet and saturated conditions are shown in Fig. 3. Unlike typical shear

Table 1 Measured values of UCS and ϕ_b and their weakening coefficients under different moisture conditions for granite and sandstone

Rock type	Moisture condition	UCS (MPa)	ϕ_b (°)	β_s (%)	β_f (%)
Granite	Dry	157.93	33.46	0	0
	Wet surface	157.93	30.59	0	8.58
	Saturated	133.97	30.38	15.17	9.51
Sandstone	Dry	76.60	35.30	0	0
	Wet surface	76.60	32.92	0	6.80
	Saturated	38.00	32.62	50.39	7.64

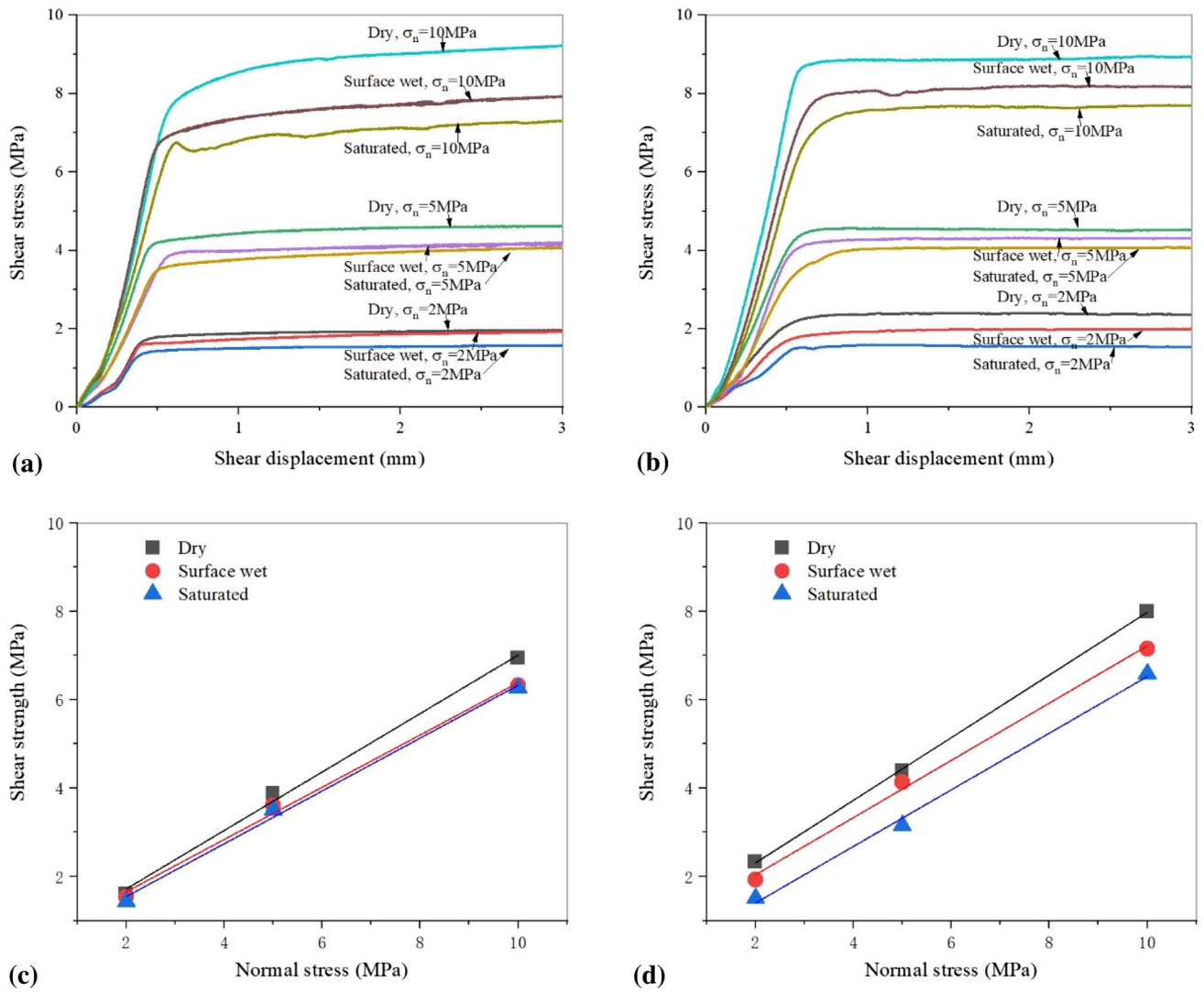


Fig. 3 Relations between shear stress and shear displacement for flat fracture samples of (a) granite and (b) sandstone under three different moisture conditions. Relations between shear strength and normal stress for flat fracture samples of (c) granite and (d) sandstone

stress—shear displacement curves of rough-walled fractures, the curves obtained from flat surface are simply composed of an increasing stage and a subsequent constant stage without obvious peaks. This constant stage represents the dynamic frictional behavior of a rock material that elevates with the increasing normal stress. The dry samples exhibit the greatest values of shear stress for all cases, followed by surface wet and saturated samples. Plotting the shear strength against the normal stress, the inclinations of the best-fitted straight lines represent the basic friction angles under the three conditions. As tabulated in Table 1, the obtained values of ϕ_b for granite are 33.46°, 30.59° and 30.38°, and for sandstone are 35.32°, 32.92° and 32.62°, under dry, surface wet and saturated conditions, respectively. The values of ϕ_b are almost identical for the tests under surface wet and saturated conditions, which

are both several degrees lower than that under dry conditions, indicating that ϕ_b is only controlled by the surface condition for the same material. Since all the sample surfaces were treated by the same method (i.e., the same level of polish), the only distinguishable factor resulting in the difference is the moisture condition. The sandstone samples exhibit greater values of ϕ_b than those of the granite due to the existence of small-scale undulations formed by the porous structure of sandstone grains. Both rock types exhibit a similar level of reduction in ϕ_b , which may also be attributed to the same preparation procedure for the samples. The values under dry and wet conditions are in concert with those determined by tilt test on cylindrical rock samples (Alejano et al. 2012). From these results, the weakening coefficients β_f were obtained as 8.58% and

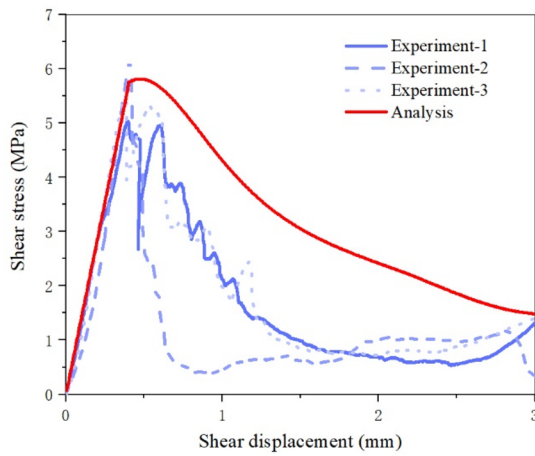
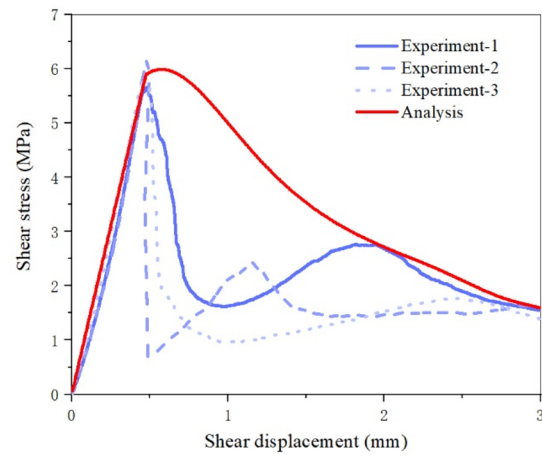
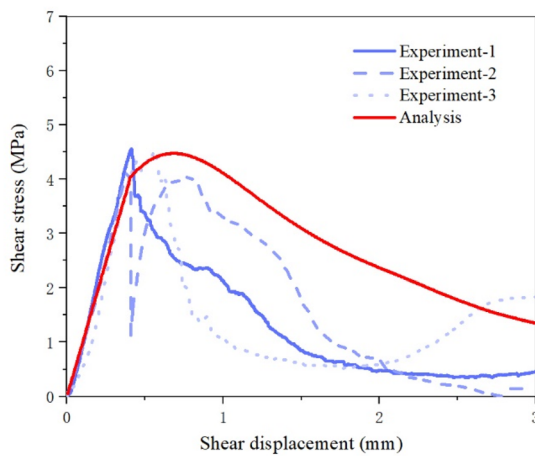
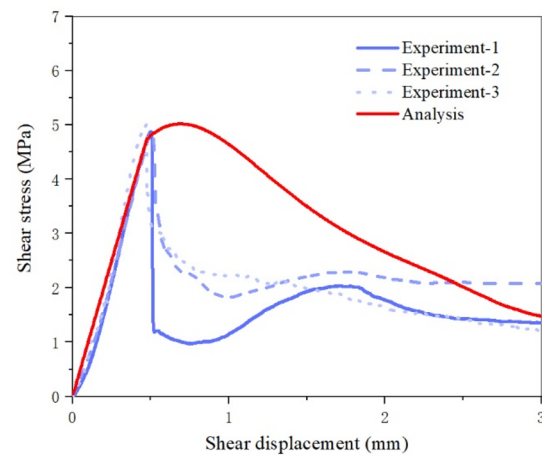
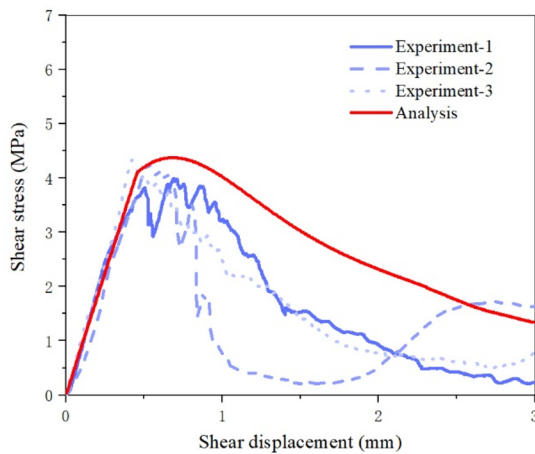
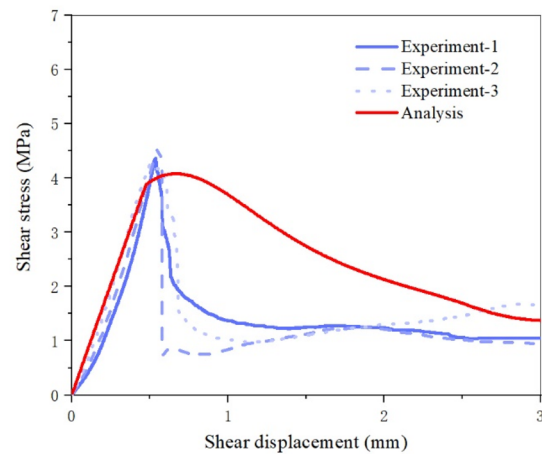
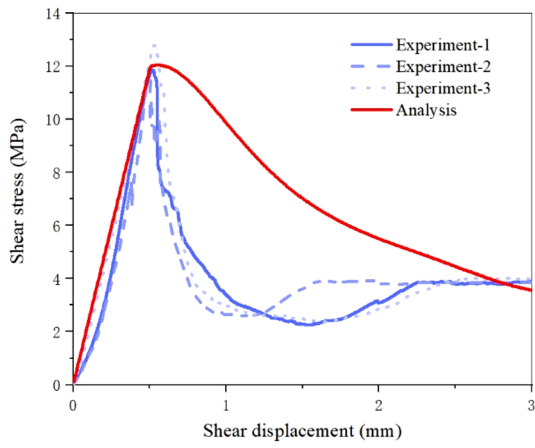
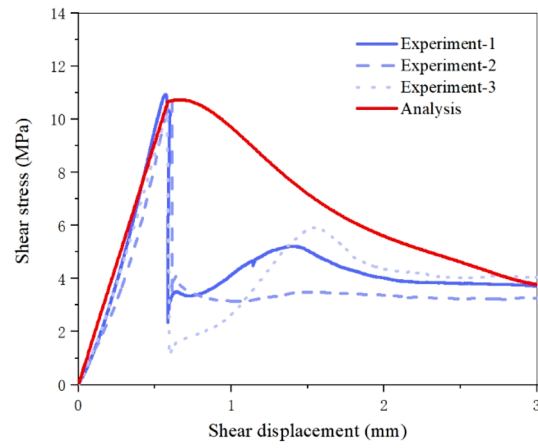
(a) Granite, dry, $\sigma_n=2$ MPa(b) Sandstone, dry, $\sigma_n=2$ MPa(c) Granite, surface wet, $\sigma_n=2$ MPa(d) Sandstone, surface wet, $\sigma_n=2$ MPa(e) Granite, saturated, $\sigma_n=2$ MPa(f) Sandstone, saturated, $\sigma_n=2$ MPa

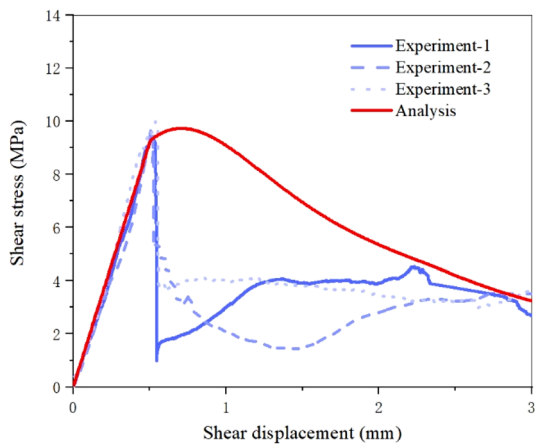
Fig. 4 Comparison of evolving shear stresses obtained from experiment and analysis during shear processes. Each experiment was repeated three times to ensure the repeatability



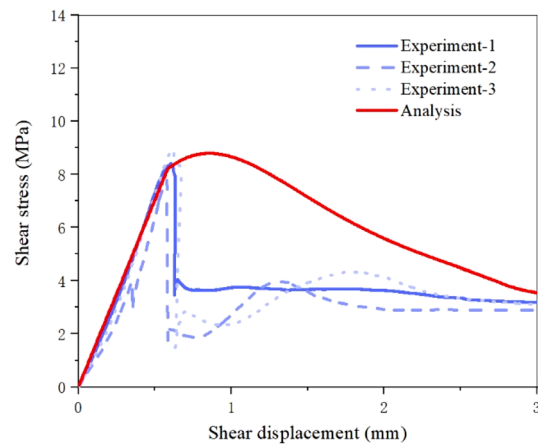
(g) Granite, dry, $\sigma_n=5$ MPa



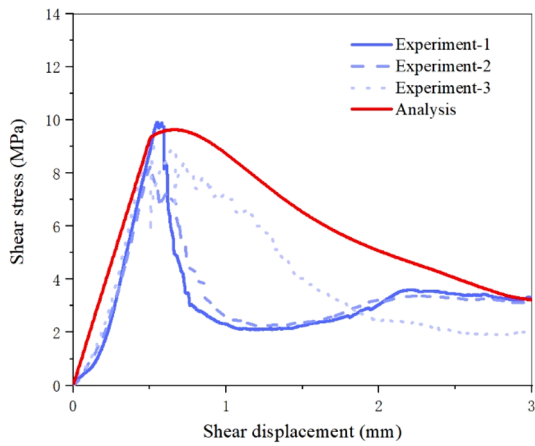
(h) Sandstone, dry, $\sigma_n=5$ MPa



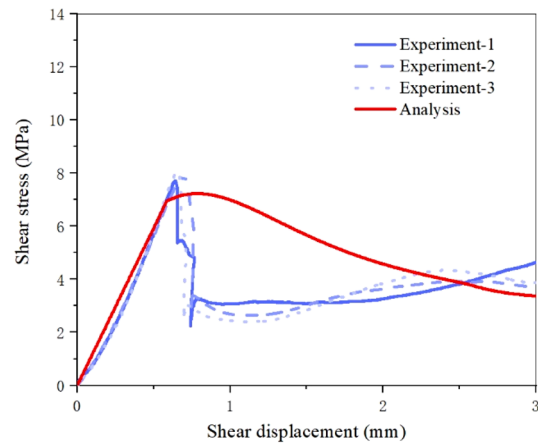
(i) Granite, surface wet, $\sigma_n=5$ MPa



(j) Sandstone, surface wet, $\sigma_n=5$ MPa



(k) Granite, saturated, $\sigma_n=5$ MPa



(l) Sandstone, saturated, $\sigma_n=5$ MPa

Fig. 4 (continued)

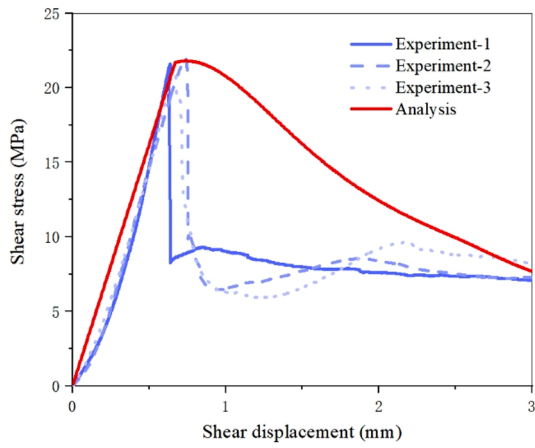
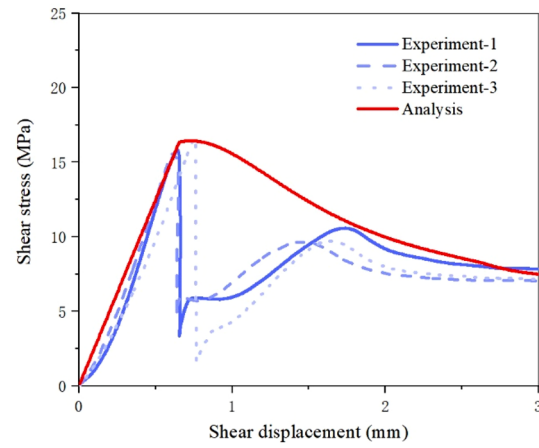
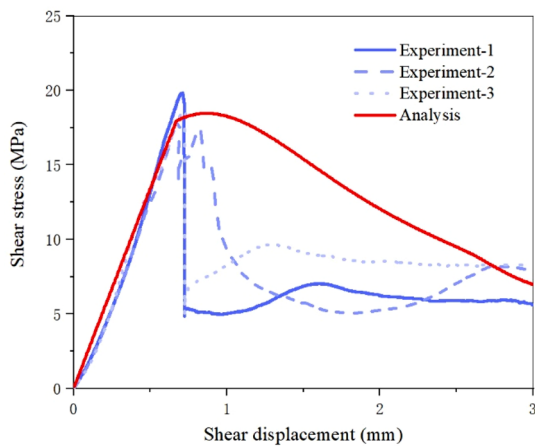
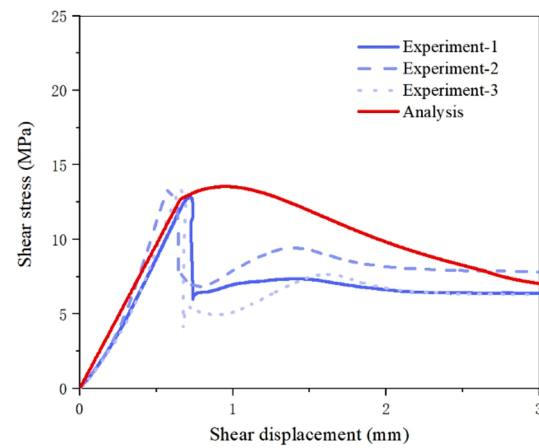
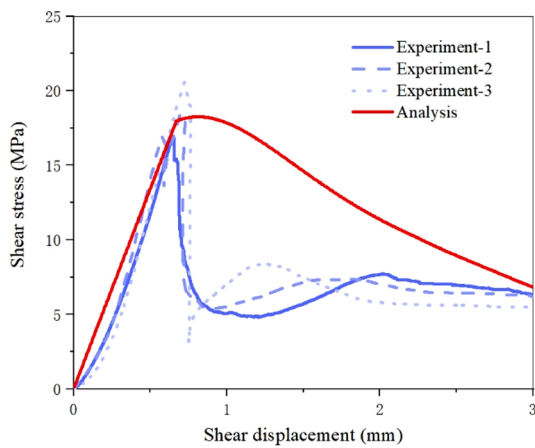
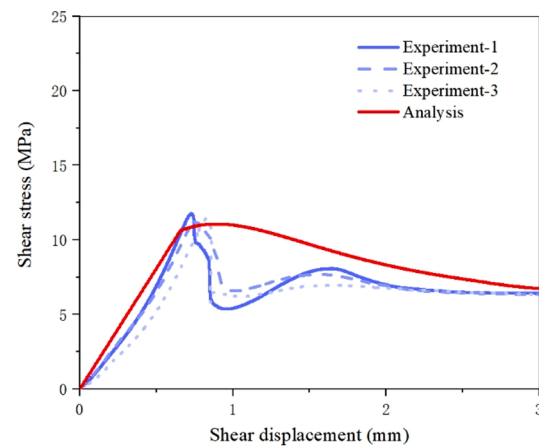
(m) Granite, dry, $\sigma_n=10$ MPa(n) Sandstone, dry, $\sigma_n=10$ MPa(o) Granite, surface wet, $\sigma_n=10$ MPa(p) Sandstone, surface wet, $\sigma_n=10$ MPa(q) Granite, saturated, $\sigma_n=10$ MPa(r) Sandstone, saturated, $\sigma_n=10$ MPa

Fig. 4 (continued)

Table 2 Measured and calculated peak and residual shear strengths for granite and sandstone under different moisture conditions

Rock type	Moisture condition	σ_n (MPa)	Measured peak shear strength (MPa)	Calculated peak shear strength (MPa)	Correlation coefficient	Measured residual shear strength (MPa)	Calculated residual shear strength (MPa)	Correlation coefficient
Granite	Dry	2	5.55	5.81	0.999	1.02	1.48	0.971
		5	12.24	12.03		3.9	2.56	
		10	21.67	21.8		7.54	7.67	
	Surface wet	2	4.39	4.47		0.81	1.35	
		5	9.73	9.73		3.28	3.24	
		10	18.81	18.46		7.28	6.98	
	Saturated	2	4.20	4.37		0.89	1.34	
		5	9.12	9.63		2.82	3.23	
		10	18.65	18.1		6	6.8	
Sandstone	Dry	2	5.91	5.99	0.996	1.52	1.59	0.991
		5	10.67	10.73		3.68	3.78	
		10	16.07	16.45		7.34	7.49	
	Surface wet	2	4.92	5.02		1.55	1.48	
		5	8.39	8.79		3.07	3.55	
		10	13.17	13.54		6.82	7.04	
	Saturated	2	4.39	4.08		1.22	1.37	
		5	7.89	7.23		4.05	3.37	
		10	11.54	11.06		6.36	6.73	

9.51% for granite, and 6.80% and 7.64% for sandstone under surface wet and saturated conditions, respectively.

4.2 Shear Behavior

The obtained values of UCS and ϕ_b under dry condition and the weakening coefficients under the other two conditions were input into the analytical model to calculate the full shear stress—shear displacement curves, which are plotted together with the experimental results as shown in Fig. 4. Here only the results of the samples with sawtooth asperities are presented. Each experiment was repeated three times to reduce the possible error. Since all the samples have identical surface characteristics, the discrepancy among the three repeated cases under each condition is considerably small and the evolutions of the shear stress during shear exhibit a similar tendency for all cases. This confirmed that steady testing results could be obtained with the experimental procedure and the apparatus employed. The shear stress increases rapidly in a nearly linear manner until reaching the peak value, after which the stress exhibits a sudden drop for most cases and gradually reaches some constant residual values. Such sudden drop is frequently observed on the failure of brittle materials, which, however, deviates from the prediction of the analytical model to some extent, which descends more gently after failure. For the sawtooth asperities, the failure may happen simultaneously on all

asperities, triggering an instantaneous drop in the shear stress as observed by the experimental measurement. In contrast, the analytical model considers a continuous yielding mechanism based on the wear theory that produces much slower descending post-failure curves. The increase in shear stress after the sudden drop as observed on the experimental results may be due to the recovery of shear stress required to slide the fracture again after failure. Despite this difference, the predictions made by the analytical model agree well with the shear stresses measured by experiment.

To quantitatively compare the analytical and experimental results, the peak and residual shear stresses of experimental and analytical results are tabulated in Table 2 and the experimental results are plotted against the normal stress as shown in Fig. 5. Here, the shear stress at the shear displacement of 3 mm was selected as the residual shear strength since the stress has reached a steady state for most cases. It is obvious that the dry samples exhibit much greater shear strength than the wetted samples, and the shear strength of the surface wet samples is slightly greater than the saturated samples. The peak shear strengths of granite and sandstone fractures are fairly close to each other at a relatively low normal stress, i.e., 2 MPa, and the difference gradually increases up to 38% at the normal stress of 10 MPa. In contrast, the residual shear strength of two rock types maintains an almost identical level regardless of the normal stress. The slopes of the bested fitted straight lines in Fig. 5 represent the peak and residual friction angles, all

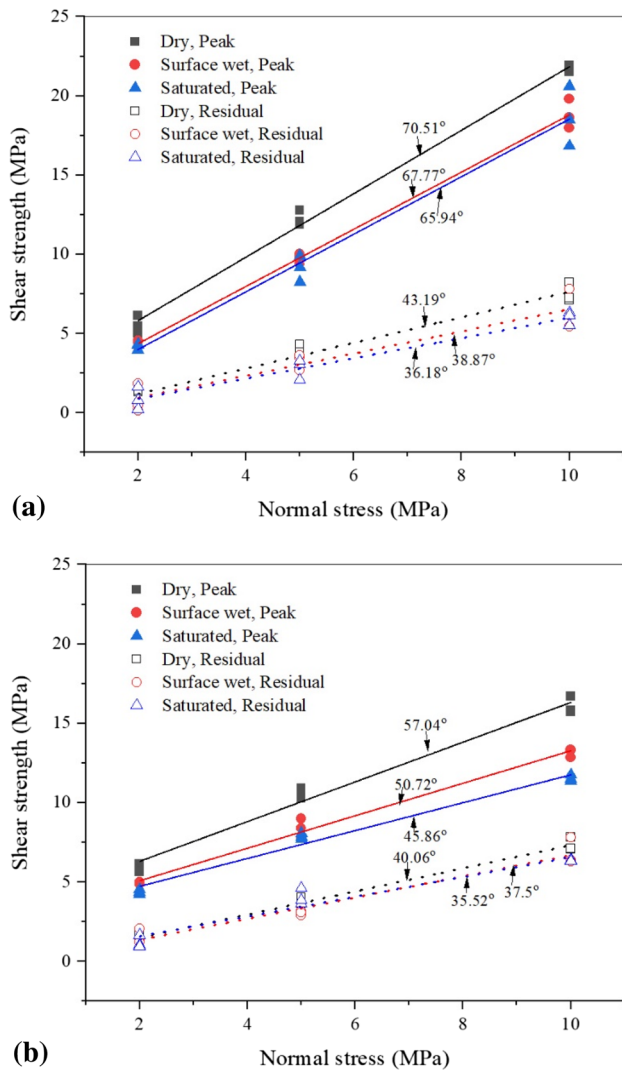


Fig. 5 Peak (solid lines) and residual (dashed lines) shear strengths versus normal stress for (a) granite and (b) sandstone obtained from experiment. The numbers are friction angles

the values of which are presented on the figure. For the friction angle at peak, the granite exhibits reductions of 2.74° – 4.57° under surface wet and saturated conditions, while the values for the sandstone range 6.32° – 11.18° , above two times greater than the granite. For the residual friction angle, two rocks exhibit a similar range of reduction (around 4.32° – 7.01°). In the residual stage, the major asperities have been efficiently sheared-off, and the residual shear stress is only mobilized by the frictional resistance of smoothed surfaces. Therefore, the residual friction angle corresponds well with the basic friction angle (Table 1), with slightly greater values because some undamaged asperities still make contributions to the shear resistance in the residual stage.

From the values in Table 2, the coefficient of correlation between the analytical and experimental results was calculated

that is greater than 0.97 for granite and sandstone, showing that the analytical model precisely predicted the peak and residual shear strengths under different moisture conditions. It also confirmed that the difference in shear strength among the three moisture conditions can be quantitatively characterized by the two weakening coefficients.

4.3 Surface Morphology After Test

Figure 6 shows the reductions of asperity heights owing to shear under normal stress of 10 MPa. By comparing the scanned fracture surface before and after direct shear testing, the total volume loss of asperities can be determined (Table 3). Obviously, the damage mainly happened at the top of each asperity. The largest loss of asperity volume occurred on the dry granite and sandstone fracture surfaces, and the loss of asperity volume became less for the fractures under surface wet or under saturated conditions. The volume of sheared-off asperities was also calculated by the analytical model, and the analytical results are generally greater than the measured values. In the measurement, we identified that a small portion of sheared-off particles adhered firmly to the surfaces by the compression in the subsequent shear process, which was not considered in the present analytical model. Such adhesion is more obvious in a wet environment, which may be responsible for the discrepancy between the experimental measurement and the analytical calculation under wet conditions.

5 Applications

5.1 Application to Rough-Walled Fractures

The sawtooth samples represent an idealized geometry of asperities, which have successfully helped in understanding the contributions of UCS and ϕ_b to the shear strength degradation by eliminating the effect of roughness as demonstrated above. We then applied the analytical model with the obtained weakening coefficients to rough-walled fractures to further verify its applicability to natural fractures. Shear test was conducted on tensile granite fractures (Fig. 1d) subject to a normal stress of 10 MPa under three moisture conditions. Tensile sandstone fractures were not considered due to the limited number of sandstone fracture samples. The splitting was stress-controlled to generate tensile fracture surfaces with similar level of roughness. The geometric characteristics of the critical waviness and critical unevenness (i.e., i_w , λ_w , α_u , and λ_u) were obtained by analyzing the digitized surfaces (Fig. 7). The testing results and the corresponding analytical results of the relations between shear stress and shear displacement are shown in Fig. 7. The peak

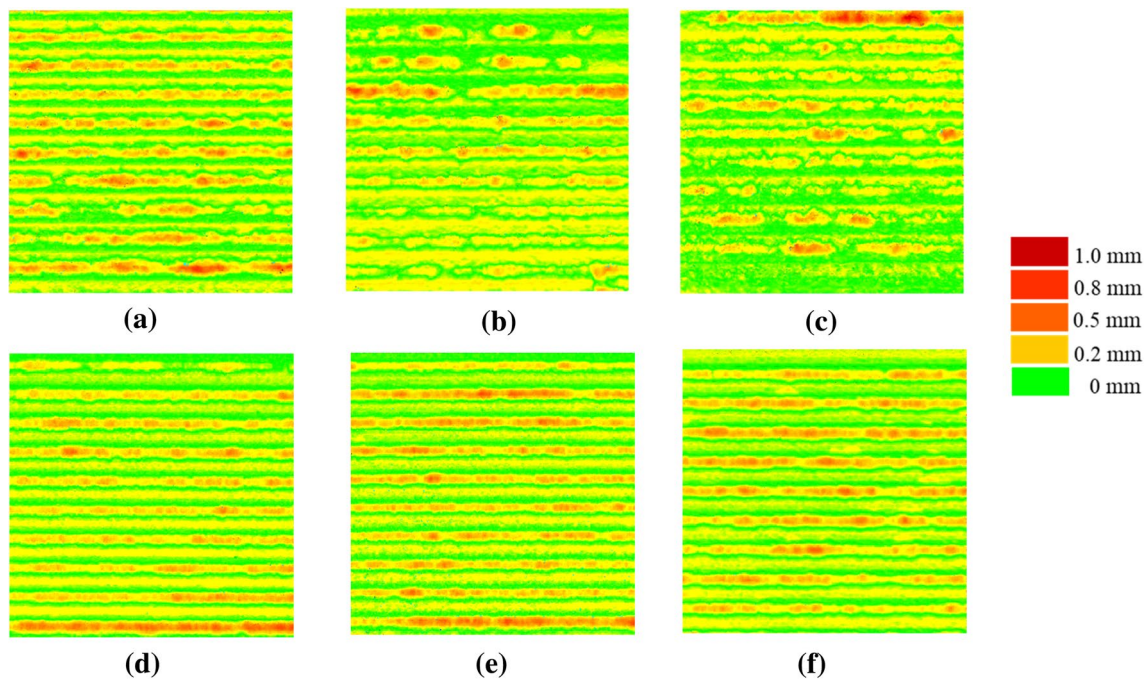


Fig. 6 Surface morphology of sawtooth fracture samples sheared under a normal stress of 10 MPa. **a, b, c** Are granite samples under dry, surface wet and saturated conditions, respectively, and **(d), (e)**

and **(f)** are sandstone samples under dry, surface wet and saturated conditions, respectively

shear stress varies in a greater range for the three repeated tests under each condition than those of the sawtooth samples due to the variations in the surface roughness. The greater values of the geometric parameters as shown in the legend, the greater the shear strength. The peak shear strength exhibits a clear descending trend under dry, surface wet and saturated conditions, analogous to the sawtooth samples, while such decline for the residual strength is not obvious. The analytical model was able to accurately predict the peak and residual shear strengths (Fig. 7d), which validated the model itself and proved again that the two weakening coefficients can efficiently represent the water-induced degradation in the shear strength of fractures.

5.2 Application to Other Rock Types

The validated model allowed us to put forward an investigation on the weakening in the shear strength of fractures of various rock types. We collected a series of experimental datasets on the UCS and ϕ_b of dry and saturated rocks of seven rock types frequently encountered in the practices. The datasets were reported by different researchers tested under different environments that exhibit a wide range for each rock type. To achieve a generic understanding, as tabulated in Table 4, the mean values of UCS and ϕ_b for each rock type under dry and saturated conditions were used to calculate the peak and residual shear strengths. The values of ϕ_b were presumed to be identical under surface wet and saturated conditions given their close values as tabulated in Table 1. Beside UCS and ϕ_b , the surface roughness plays an important role in the shear strength. Here, we calculated four levels of the inclination angle of the major asperities (waviness), i.e., 10°, 20°, 30° and 40° to parametrically study its influence. A constant value of 4 mm was assigned to the wavelength and the unevenness is neglected since its contribution to the shear strength is far smaller than that of the waviness (Li et al. 2018).

Table 3 Sheared-off volume of granite and sandstone fracture surfaces under different moisture conditions

Rock type	Moisture condition	Measured	Calculated
Granite	Dry	361.65	370.41
	Surface wet	331.57	361.78
	Saturated	310.15	374.41
Sandstone	Dry	403.36	440.53
	Surface wet	390.59	433.53
	Saturated	359.58	445.70

Figure 8 shows the predicted values of the peak and residual frictional coefficients for seven types of rock fractures. The typical sedimentary rocks as mudstone and shale exhibit the lowest fracture shear strength while the metamorphic

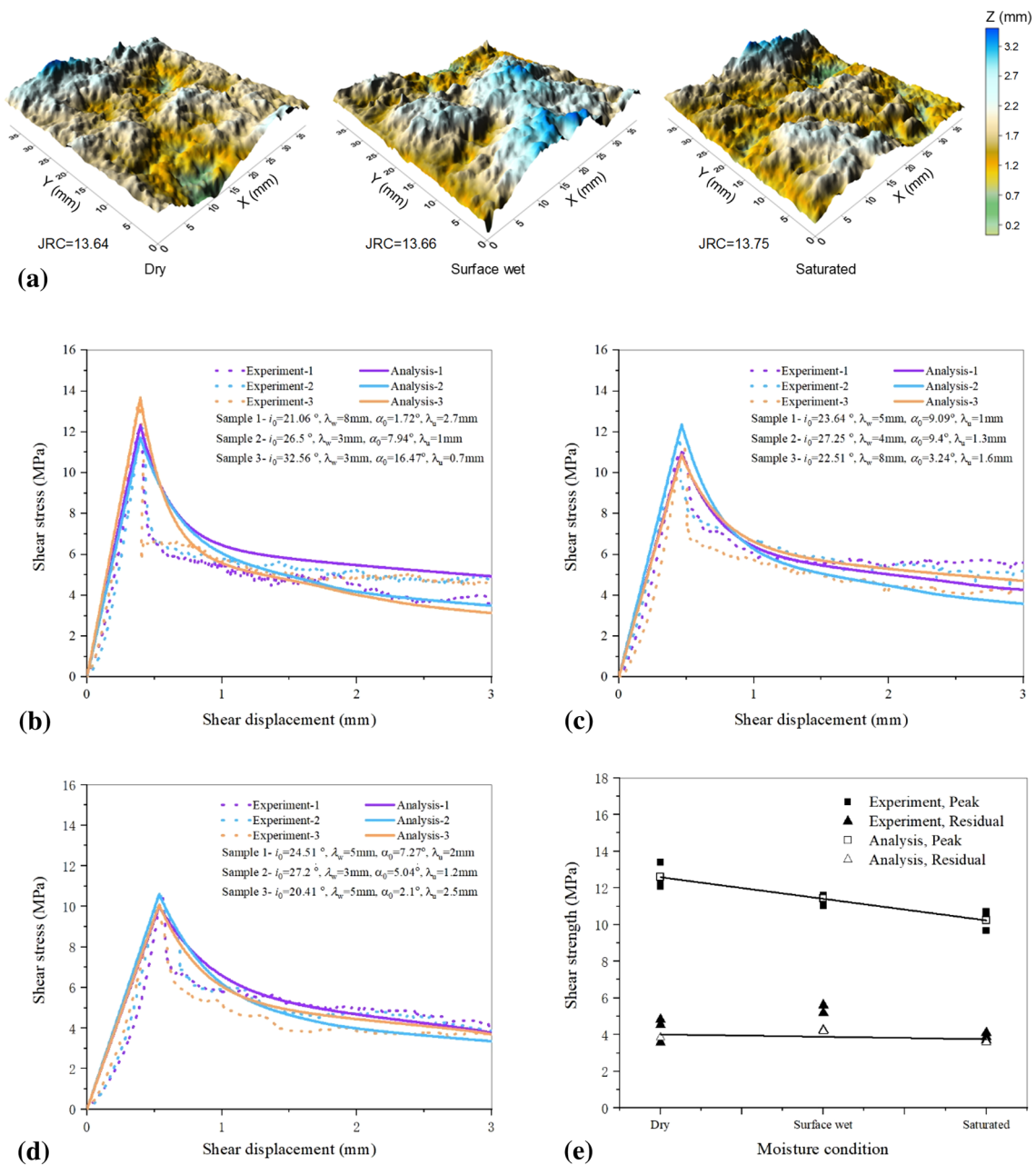


Fig. 7 a Representative surface morphology of the tested rough fractures and their JRC values. Relations between shear stress and shear displacement under (b) dry, (c) surface wet, (d) saturated conditions

for tensile granite fractures sheared at a normal stress of 10 MPa and their comparison with the analytical results. e The peak and residual shear strengths under three moisture conditions

rocks the greatest, which are in line with the general strength properties of rocks. Different rocks also exhibit different degradation behaviors under surface wet and saturated conditions due to the comparative contributions of the reductions in UCS and ϕ_b to the peak shear strength. For instance, the strength degradation is primarily controlled by the reduction in ϕ_b for marble, while it is controlled by the reduction in UCS for sandstone (Table 4). The most obvious reduction happens when the inclination angle i_0 changes from 10° to

20° for granite, while the maximum occurs when i_0 changes from 30° to 40°. This difference is attributed to the different yielding behaviors controlled by the relative magnitudes of UCS, ϕ_b and i_0 , that can be realistically characterized by the developed analytical model as validated by the experimental results. The residual frictional coefficients are almost identical when sheared under surface wet and saturated conditions due to their identical values of ϕ_b , which are lower than that under dry conditions in different degrees. The inclination

Table 4 Collected experimental datasets of UCS and ϕ_b for dry and saturated rocks from literature

Rock type	UCS (MPa)		β_s (%)	References	ϕ_b (°)		β_f (%)	References
	Dry	Saturated			Dry	Wet		
Mudstone	51.38	8.31	83.83	Lashkaripour and Ajalloeian (2000) Erguler and Ulusay (2009) Jiang et al. (2014) Lu et al. (2017)	32	29	9.38	Barton (1973) Alejano et al. (2012)
Siltstone	62.24	31.01	50.18	Vasarhelyi (2005) Erguler and Ulusay (2009) Zhang et al. (2017)	32	30	6.25	
Limestone	37.8	24.71	34.63	Howarth (1987) Rajabzadeh et al. (2012)	34	31	8.82	
Sandstone	77.23	52.76	31.68	Hawkins (1998) Vasarhelyi (2003) Shukla et al. (2013) Verstryngge et al. (2014)	31	29	6.45	
Marble	67.35	50.94	24.37	Howarth (1987) Rajabzadeh et al. (2012)	49	42	14.29	
Shale	83.89	29.98	64.26	Lashkaripour and Ajalloeian (2000) Bian et al. (2019) Liu et al. (2018)	29	21	27.59	
Granite	146.61	124.79	14.88	Lajtai et al. (1987)	33	31	6.06	

angle has negligible influences on the residual frictional coefficient because it is primarily a material property rather than a geometric property, analogous to ϕ_b . For granite and sandstone, the estimated peak and residual frictional coefficients using the data from the literature are in good agreement with the obtained values in this study. This indicates that Fig. 8 can serve as a first approximation for wetting-induced weakening of rock fractures. It is notable that the above estimation did not consider the scale effect of fractures, which can significantly influence the shear strength. Previous studies have revealed a descending trend for the shear strength with the increasing fracture size and corresponding analytical/empirical models have been established to account for this effect (Barton et al. 1985; Vallier et al. 2010; Tatone and Grasselli 2013; Hencher and Richards 2014). Therefore, these results need to be utilized in conjunction with reasonable scale laws when different fracture sizes are encountered.

6 Conclusions

Direct shear tests were conducted on granite and sandstone fractures under dry, surface wet and saturated conditions to investigate the effect of moisture condition on the shear strength degradation. The variations in the UCS and ϕ_b were experimentally constrained, which were transformed into two weakening coefficients to quantify the degradations in

the strength of contacting asperities and the basic frictional resistance. The weakening coefficients were then incorporated into an analytical model that characterizes the entire stress evolution during shear based on wear theory to estimate the shear strength under different moisture conditions.

The results revealed that the peak and residual shear strengths exhibit a monotonic descending trend from dry to surface wet and then saturated conditions. The difference in the shear strength between dry and surface wet conditions originates from the lubricant effect of water that can be represented by the change in ϕ_b with a weakening coefficient less than 10% for both rocks. Under the saturated condition, the weakening coefficient of the UCS varies significantly from 15.17% for granite to 50.39% for sandstone, which combined with the reduction in ϕ_b results in further degradation of the shear strength. It is obvious that the friction angle at peak is not a simple combination of ϕ_b and the slope of major asperities, and the yielding and failure mechanisms of contacting asperities need to be taken into account, which is realized by the analytical model that calculates the shear stress evolution based on the classic wear theory. The model is able to precisely capture the peak and residual shear strengths and provides a rough agreement with the measured sheared-off volumes under different moisture conditions.

For other rocks, although the weakening coefficient of ϕ_b is unlikely to become greater than 27.59%, the reduction in UCS spans a wide range from 14.88% for granite to 83.83% for mudstone. For crystalline rocks that suffer from

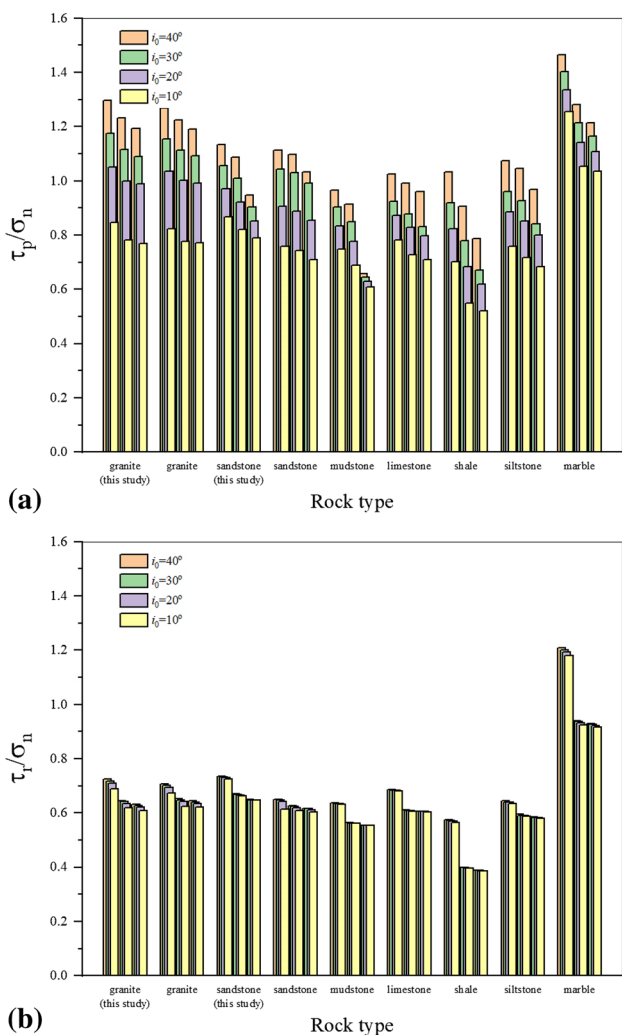


Fig. 8 The values of the peak frictional coefficient (a) and residual frictional coefficient (b) for seven types of rock fractures calculated under four different slope angles of waviness. For each group of columns, the left represents dry, the center represents surface wet and the right represents saturated conditions. Results of granite and sandstone tested in the study are plotted for comparison

a relatively smaller degradation in the UCS, the water-mediated lubrication seems to be the primary mechanism reducing the shear strength as suggested by Eq. (1) and the results. While for sedimentary rocks, particularly clay-rich rocks, the remarkable degradation in UCS may dominate the weakening in the shear strength since the variation in ϕ_b is relatively gentle among different rocks. In practices, the values of UCS and ϕ_b of rocks under different moisture conditions can be steadily obtained via well-established experiment methods as suggested by ISRM (Ulusay 2016), which could help obtain the weakening coefficients. With the developed analytical approach, the shear strength of rock fractures and the magnitude of water-induced

weakening could be accurately estimated that may contribute to the efficient and economic engineering works.

Acknowledgements This study was financially supported by the National Natural Science Foundation of China (No. 51739006, 51609136, 51779123) and Natural Science Foundation of Zhejiang Province, China (No. LR19E090001). These supports are gratefully acknowledged. The testing results and the surface morphology data of fractures are available at the corresponding author.

Compliance with Ethical Standards

Conflict of interest We declare no conflict of interest.

References

Alejano LR, González Javier, Muralha José (2012) Comparison of different techniques of tilt testing and basic friction angle variability assessment. *Rock Mech Rock Eng* 45(6):1023–1035

Barton N (1971) A relationship between joint roughness and joint shear strength. In: *Proceedings of international symposium on rock fracture*. 1–8

Barton N (1973) Review of a new shear-strength criterion for rock joints. *Eng Geol* 7(4):287–332

Barton N (1982) Modelling rock joint behavior from in situ block tests: implications for nuclear waste repository design. Office of Nuclear Waste Isolation, Columbus

Barton N, Choubey V (1977) The shear strength of rock joints in theory and practice. *Rock Mech* 10(1–2):1–54

Barton N, Bandis S, Bakhtar K (1985) Strength, deformation and conductivity coupling of rock joints. *Int J Rock Mech Min Sci Geomech Abstr* 22(3):121–140

Barwell FT (1958) Report on papers on wear presented at the institution of mechanical engineers conference. *Wear* 1(5):418–445

Baud P, Zhu W, Wong TF (2000) Failure mode and weakening effect of water on sandstone. *J Geophys Res* 105:16371–16389

Bian K, Liu J, Zhang W, Zheng X, Ni S, Liu Z (2019) Mechanical behavior and damage constitutive model of rock subjected to water-weakening effect and uniaxial loading. *Rock Mech Rock Eng* 52(1):97–106

Chen Y, Cao P, Mao D, Pu C, Fan X (2014) Morphological analysis of sheared rock with water–rock interaction effect. *Int J Rock Mech Min Sci* 70:264–272

Cherblanc F, Berthouneau J, Bromblet P, Huon V (2016) Influence of water content on the mechanical behavior of limestone: role of clay minerals content. *Rock Mech Rock Eng* 49:2033–2042

Ciantia MO, Castellanza R, Crosta G, Hueckel T (2015a) Effects of mineral suspension and dissolution on strength and compressibility of soft carbonate rocks. *Eng Geol* 184:1–18

Ciantia MO, Castellanza R, Prisco C (2015b) Experimental study on the water-induced weakening of calcarenites. *Rock Mech Rock Eng* 48:441–461

Dove Patricia M (1995) Geochemical controls on the kinetics of quartz fracture at subcritical tensile stresses. *J Geophys Res* 100(B11):22349–22359

Erguler ZA, Ulusay R (2009) Water-induced variations in mechanical properties of clay-bearing rocks. *Int J Rock Mech Min Sci* 46(2):355–370

Feng XT, Chen S, Li S (2001) Effects of water chemistry on microcracking and compressive strength of granite. *Int J Rock Mech Min Sci* 38(4):557–568

Feucht LJ, Logan JM (1990) Effects of chemically active solutions on shearing behavior of a sandstone. *Tectonophysics* 175(1):159–176

- Grasselli G, Wirth J, Egger P (2002) Quantitative three-dimensional description of a rough surface and parameter evolution with shearing. *Int J Rock Mech Min Sci* 39(6):789–800
- Gutierrez M, øIno LE, Nygård R (2000) Stress-dependent permeability of a de-mineralised fracture in shale. *Mar Pet Geol* 17(8): 0–907
- Hawkins AB (1998) Aspects of rock strength. *Bull Eng Geol Env* 57:17–30
- Hencher SR, Richards LR (2014) Assessing the shear strength of rock discontinuities at laboratory and field scales. *Rock Mech Rock Eng* 48:883–905
- Howarth DF (1987) The effect of pre-existing microcracks on mechanical rock performance in sedimentary and crystalline rocks. *Int J Rock Mech Min Sci Geomech Abstr* 24:223–233
- Hua W, Dong S, Li Y, Wang Q (2016) Effect of cyclic wetting and drying on the pure mode II fracture toughness of sandstone. *Eng Fract Mech* 153:143–150
- Indraratna B, Welideniya HS, Brown ET (2005) A shear strength model for idealised infilled joints under constant normal stiffness. *Géotechnique* 55(3):215–226
- Indraratna B, Thirukumaran S, Brown ET, Zhu SP (2015) Modelling the shear behaviour of rock joints with asperity damage under constant normal stiffness. *Rock Mech Rock Eng* 48(1):179–195
- Itasca Consulting Group Inc. (2011), UDEC (Universal Distinct Element Code) Version 5.0
- Jaeger JC, Cook NGW, Zimmerman RW (2007) *Fundamentals of rock mechanics*, 4th edn. Blackwell, Oxford
- Jiang Q, Cui J, Feng X, Jiang Y (2014) Application of computerized tomographic scanning to the study of water-induced weakening of mudstone. *Bull Eng Geol Env* 73(4):1293–1301
- Karfakis MG, Akram M (1993) Effects of chemical solutions on rock fracturing. *Int J Rock Mech Min Sci Geomech Abstr* 30(7):1253–1259
- Kim T, Jeon S (2019) Experimental study on shear behavior of a rock discontinuity under various thermal, hydraulic and mechanical conditions. *Rock Mech Rock Eng* 52:2207–2226
- Lajtai EZ, Schmidtke RH, Bielus LP (1987) The effect of water on the time-dependent deformation and fracture of a granite. *Int J Rock Mech Min Sci Geomech Abstr* 24(4):247–255
- Lashkaripour GR, Ajalloeian R (2000). The effect of water content on the mechanical behaviour of fine-grained sedimentary rocks. In: *ISRM International Symposium*, 19–24 November, Melbourne, Australia
- Li N, Zhu YM, Su B, Gunter S (2003) A chemical damage model of sandstone in acid solution. *Int J Rock Mech Min Sci* 40(2):243–249
- Li Z, Sheng Y, Reddish DJ (2005) Rock strength reduction and its potential environmental consequences as a result of groundwater rebound. In: *The 9th international mine water association congress*, Oviedo, Spain
- Li B, Jiang Y, Koyama T, Jing L, Tanabashi Y (2008) Experimental study of the hydro-mechanical behavior of rock joints using a parallel-plate model containing contact areas and artificial fractures. *Int J Rock Mech Min Sci* 45(3):362–375
- Li Y, Oh J, Mitra R, Canbulat I (2017) A fractal model for the shear behaviour of large-scale opened rock joints. *Rock Mech Rock Eng* 50(1):67–79
- Li Y, Wu W, Li B (2018) An analytical model for two-order asperity degradation of rock joints under constant normal stiffness conditions. *Rock Mech Rock Eng* 1:1–15
- Liu J, Sheng J, Polak A, Elsworth D, Yasuhara H, Grader A (2006) A fully-coupled hydrological-mechanical-chemical model for fracture sealing and preferential opening. *Int J Rock Mech Min Sci* 43:23–36
- Liu D, Wang Z, Zhang X, Wang Y, Zhang X, Li D (2018) Experimental investigation on the mechanical and acoustic emission characteristics of shale softened by water absorption. *J Nat Gas Sci Eng* 50:301–308
- Lockner DA (1995) *Rock failure. Rock physics & phase relations: a handbook of physical constants*. American Geophysical Union, Washington, pp 127–147
- Lu Y, Wang L, Sun X, Wang J (2017) Experimental study of the influence of water and temperature on the mechanical behavior of mudstone and sandstone. *Bull Eng Geol Env* 76(2):645–660
- Min KB, Rutqvist J, Elsworth D (2009) Chemically and mechanically mediated influences on the transport and mechanical characteristics of rock fractures. *Int J Rock Mech Min Sci* 46:80–89
- Nara Y, Hiroyoshi N, Yoneda T, Kaneko K (2010) Effects of relative humidity and temperature on subcritical crack growth in igneous rock. *Int J Rock Mech Min Sci* 47(4):640–646
- Pellet FL, Keshavarz M, Boulon M (2013) Influence of humidity conditions on shear strength of clay rock discontinuities. *Eng Geol* 157:33–38
- Qiao L, Wang Z, Huang A (2017) Alteration of mesoscopic properties and mechanical behavior of sandstone due to hydro-physical and hydro-chemical effects. *Rock Mech Rock Eng* 50:255–267
- Queener CA, Smith TC, Mitchell WL (1965) Transient wear of machine parts. *Wear* 8(5):391–400
- Rajabzadeh MA, Moosavinasab Z, Rakhshandehroo G (2012) Effects of rock classes and porosity on the relation between uniaxial compressive strength and some rock properties for carbonate rocks. *Rock Mech Rock Eng* 45(1):113–122
- Saeb S, Amadei B (1992) Modelling rock joints under shear and normal loading. *Int J Rock Mech Min Sci Geomech Abstr* 29(3):267–278
- Shukla R, Ranjith PG, Choi SK, Haque A, Yellishetty M, Hong L (2013) Mechanical behaviour of reservoir rock under brine saturation. *Rock Mech Rock Eng* 46(1):83–93
- Tatone BSA, Grasselli G (2013) An investigation of discontinuity roughness scale dependency using high-resolution surface measurements. *Rock Mech Rock Eng* 46(4):657–681
- Ulusay R (2016) *The ISRM Suggested methods for rock characterization, testing and monitoring: 2007–2014*, ISRM, Springer, Switzerland
- Ulusay R, Hudson JA (2007) *The complete ISRM suggested methods for rock characterization, testing and monitoring: 1974–2006*, ISRM, Springer, Switzerland.
- Ulusay R, Karakul H (2016) Assessment of basic friction angles of various rock types from turkey under dry, wet and submerged conditions and some considerations on tilt testing. *Bull Eng Geol Env* 75(4):1683–1699
- Vallier F, Mitani Y, Boulon M, Esaki T, Pellet F (2010) A shear model accounting scale effect in rock joints behavior. *Rock Mech Rock Eng* 43(5):581–595
- Van Eeckhout EM (1976) The mechanisms of strength reduction due to moisture in coal mine shales. *Int J Rock Mech Min Sci Geomech Abstr* 13:61–67
- Vasarhelyi B (2003) Some observations regarding the strength and deformability of sandstones in dry and saturated conditions. *Bull Eng Geol Env* 62(3):245–249
- Vasarhelyi B (2005) Statistical analysis of the influence of water content on the strength of the miocene limestone. *Rock Mech Rock Eng* 38:69–76
- Verstrynge E, Adriaens R, Elsen J, Van Balen K (2014) Multi-scale analysis on the influence of moisture on the mechanical behavior of ferruginous sandstone. *Constr Build Mater* 54:78–90
- Wasantha PLP, Ranjith PG (2014) Water-weakening behavior of Hawkesbury sandstone in brittle regime. *Eng Geol* 178:91–101
- Wong LNY, Maruvanchery V, Liu G (2016) Water effects on rock strength and stiffness degradation. *Acta Geotech* 11:713–737
- Yasuhara H, Elsworth D, Polak A (2004) Evolution of permeability in a natural fracture: significant role of pressure solution. *J Geophys Res* 109:B03204

- Zhang D, Pathegama Gamage R, Perera M, Zhang C, Wanniarachchi W (2017) Influence of water saturation on the mechanical behaviour of low-permeability reservoir rocks. *Energies* 10(2):236
- Zhao Z, Yang J, Zhang D, Peng H (2017a) Effects of wetting and cyclic wetting-drying on tensile strength of sandstone with a low clay mineral content. *Rock Mech Rock Eng* 50:485–491
- Zhao Z, Yang J, Zhou D, Chen Y (2017b) Experimental investigation on the wetting-induced weakening of sandstone joints. *Eng Geol* 225:61–67
- Zhao Z, Guo T, Ning Z, Dou Z, Dai F, Yang Q (2018a) Numerical modeling of stability of fractured reservoir bank slopes subjected to water-rock interactions. *Rock Mech Rock Eng* 51:2517–2531
- Zhao Z, Peng H, Wu W, Chen YF (2018b) Characteristics of shear-induced asperity degradation of rock fractures and implications for solute retardation. *Int J Rock Mech Min Sci* 105:53–61
- Zhao C, Niu J, Zhang Q, Zhao C, Zhou Y (2019a) Failure characteristics of rock-like materials with single flaws under uniaxial compression. *Bull Eng Geol Env* 78(1):593–603
- Zhao Z, Dou Z, Xu H, Liu Z (2019b) Shear behavior of Beishan granite fractures after thermal treatment. *Eng Fract Mech* 213:223–240
- Zou L, Jing L, Cvetkovic V (2015) Roughness decomposition and non-linear fluid flow in a single rock fracture. *Int J Rock Mech Min Sci* 75:102–118

Publisher's Note Springer Nature remains neutral with regard to jurisdictional claims in published maps and institutional affiliations.